

# In vivo evaluation of bending strengths and degradation rates of different magnesium pin designs for oral stapler

Journal of Applied Biomaterials &  
Functional Materials  
18: 1–10  
© The Author(s) 2020  
Article reuse guidelines:  
sagepub.com/journals-permissions  
DOI: 10.1177/2280800019836400  
journals.sagepub.com/home/jbf  
 SAGE

Wenjun Li<sup>1,2</sup> , Fusong Yuan<sup>1,2</sup>, Jing Bai<sup>3</sup>, Junyao Cheng<sup>3</sup>,  
Hongxiang Li<sup>4</sup>, Jianqiao Zheng<sup>1,2</sup>, Wei Bai<sup>5</sup> and Peijun Lyu<sup>1,2</sup>

## Abstract

Magnesium alloys have been potential biodegradable implants in the areas of bone, cardiovascular system, gastrointestinal tract, and so on. The purpose of this study is to evaluate Mg–2Zn alloy degradation as a potential suture material. The study included Sprague–Dawley (SD) rats in vivo. In 24 male SD rats, tests in the leg muscle were conducted using traditional surgical incision and insertion of magnesium alloys of different designs into the tissue. The material degradation topography, elemental composition, and strength of the pins were analyzed. This paper explores magnesium pins with different cross-sectional shapes and diameters to establish a suitable pin diameter and shape for use as an oral stapler, which must have a good balance of degradation rate and strength. The results showed there were good bending strengths over different degradation periods in groups with diameters of 0.8 mm and 0.5 mm, and no significantly different bending strength between the groups of triangle and round cross-section shapes with same diameter of 0.3 mm, although the degradation rate still needs to be improved.

## Keywords

Magnesium pin, dimension, shape, degradation topography, bending strength

Date received: 18 December 2018; revised: 19 January 2019; accepted: 16 February 2019

## Introduction

The oral cavity has certain particularities: a narrow and deep cavity which is inconvenient for operation; a great oral immune system including saliva defense, oral mucosa defense, and oral lymphoid tissue; a strong healing ability and a strong regeneration ability of mucosa.<sup>1</sup>

There is high demand for oral sutures, such as tooth extraction sockets, periodontal flaps, planting flaps, and other surgeries. In oral surgery, sutures are mostly comprised of absorbable or non-absorbable macromolecular materials. Non-absorbable sutures need to be removed later and cause secondary pain as they are non-degradable. Absorbable sutures are widely used for subcutaneous tissue such as muscle, blood vessels, and the peritoneum. Commonly used materials are catgut sutures, synthetic fiber sutures, and pure natural collagen sutures. However, most absorbable sutures could cause foreign-body and

inflammatory reactions due to pieces of material degradation, monomer, catalyst release, and cell apoptosis products, which cause poor wound healing and big trauma to

<sup>1</sup>Center of Digital Dentistry, Peking University School and Hospital of Stomatology, Beijing, China

<sup>2</sup>Research Center of Engineering and Technology for Digital Dentistry, Ministry of Health, Beijing, China

<sup>3</sup>School of Materials Science and Engineering, Southeast University, Nanjing, China

<sup>4</sup>State Key Laboratory for Advanced Metals and Materials, University of Science and Technology Beijing, China

<sup>5</sup>Dental Medical Devices Testing Center, Peking University School of Stomatology, Beijing, China

### Corresponding author:

Peijun Lyu, Research Center of Engineering and Technology for Digital Dentistry, Ministry of Health, 22 Zhongguancun Nandajie, Haidian District, 100081 Beijing, PR China.  
Email: kqlpj@bjmu.edu.cn



Creative Commons Non Commercial CC BY-NC: This article is distributed under the terms of the Creative Commons

Attribution-NonCommercial 4.0 License (<http://www.creativecommons.org/licenses/by-nc/4.0/>) which permits non-commercial use, reproduction and distribution of the work without further permission provided the original work is attributed as specified on the SAGE and Open Access pages (<https://us.sagepub.com/en-us/nam/open-access-at-sage>).

patients. In addition, the strength of absorbable sutures makes it difficult to satisfy the requirement of high-strain wounds. Thus, it may be difficult for absorbable sutures to meet clinical requirements, but an easy way to suture without needing to remove stitches is critical.

Recently, some novel suture methods have included staplers, zips,<sup>2</sup> and tissue adhesives.<sup>3</sup> For example, Chen et al. reported that a surgical zipper technique achieved similar incidence of postoperative complications, less time for incision closure, and perfect aesthetic results compared with intracutaneous sutures.<sup>2</sup> Bahouth et al. proved that bovine serum albumin–glutaraldehyde tissue adhesive (BioGlue<sup>(R)</sup>) for tumor bed closure enabled satisfactory functional outcome and could potentially reduce ischemia time.<sup>3</sup> Staplers are used in some medical surgeries. For example, skin staplers are used for skin sutures such as neck or belly wounds, whereas rectal anastomosis staplers are used for gastrointestinal tract sutures.<sup>4</sup> Stapling materials are mostly stainless steel or titanium. Polyglycolic acid subcuticular absorbable staples are available for skin closure,<sup>5,6</sup> but the adverse tissue reaction and the time of closure are greater than for metallic staples.<sup>5</sup>

Biodegradable metals appear to possess adequate biocompatibility, mechanical properties, and corrosion stability to replace biodegradable polymeric sutures. Iron and its alloys have high strength, but the biodegradation rate is slow and biocompatibility of the corrosion product is controversial.<sup>7</sup> Zinc is a vital metal element in the human body and has good biocompatibility, but pure zinc is brittle and low strength, while Zn-based alloys have problems such as the stress shielding effect and non-uniform corrosion.<sup>8</sup> Magnesium matrix materials showed some advantages in terms of low density, good biocompatibility,<sup>9,10</sup> biodegradability,<sup>11</sup> high strength and modulus,<sup>12</sup> and good dimensional stability. Numerous studies have shown that Mg and its alloys have great properties of biocompatibility and biodegradation when compared to other metallic materials and have better mechanical strength compared to degradable polymeric materials.<sup>13</sup> Okawachi et al. showed that Mg may be beneficial for adhering fiber cells to surfaces and prompting cellular vitality and activity.<sup>14</sup> Most importantly, corrosion of Mg is non-toxic and can be excreted harmlessly through urine.<sup>9,11</sup>

Magnesium matrix materials have been widely studied in many medical fields.<sup>7,15–18</sup> Mg implants have been made to evaluate the treatment of patients using Mg medical devices in bone and ligament healing,<sup>19–21</sup> gastrointestinal anastomosis,<sup>22</sup> biliary tract anastomosis,<sup>16</sup> cardiovascular stents,<sup>17,18</sup> laryngeal applications,<sup>23</sup> compressed sciatic nerves repair,<sup>24</sup> and so on. For example, in bone surgery, Han et al. proved that a high-purity Mg screw showed good osseointegration and increased bone mineral density and thus has great potential for internal fixation devices in intra-articular fracture operations.<sup>25</sup> Yu et al. suggested a potential clinical application of Mg–Ag–Y

alloy rods for use as a resorbable bone fixation implant.<sup>20</sup> Magnesium wires have also been reported as being tried in bone fixation and nerves/muscle suture.<sup>7,8</sup> In cardiovascular surgery, Moravej and Mantovani showed that the role of stenting is temporary and limited to a period of 6–12 months after implantation,<sup>17</sup> and magnesium is a potential alternative material for the currently used permanent cardiovascular stents. In laryngeal microsurgery, Chng et al.,<sup>23,26</sup> by *in vitro* and *in vivo* testing, showed a clip which was held securely to the vocal fold mucosa. In hepatobiliary surgery, Yoshida et al. demonstrated a novel magnesium alloy clip that provided a sufficient sealing capability for the cystic duct and proper biodegradability in canine models.<sup>16</sup> In gastrointestinal anastomosis, Wu et al. proved that the *in vivo* implantation showed good biocompatibility of the modified Mg staples,<sup>22</sup> without inflammatory reaction, leaking, and bleeding, and the staples exhibited no fracture or severe corrosion cracks during the degradation.

There are many ways to moderate the properties of magnesium. Aluminum and rare earth elements have potential side effects on health.<sup>27</sup> Instead, zinc has been considered as an appropriate candidate due to its properties in cell functions and mechanical strength.<sup>28</sup> By modifying the proportion of zinc, we can produce different mechanical properties.<sup>29,30</sup> A lower zinc content will produce lower strength but increased tenacity. It also has good biocompatibility with Mg-based alloys.<sup>31</sup> Yan et al. proved that the Mg–6Zn alloy promoted healing and reduced inflammation by upregulating the transforming growth factor beta 1, vascular endothelial growth factor, and the basic fibroblast growth factor.<sup>32</sup> Wang et al. showed that the Mg–6Zn alloy also enhanced the expression of collagen I/III, leading to more mature collagen formation in the anastomosis.<sup>33</sup> Surface modification of magnesium can also change the degradation rate,<sup>34,35</sup> surface chemical composition, cell adhesion,<sup>10</sup> and so on.<sup>36</sup> For example, the addition of Sn or F increases the resistance to degradation,<sup>35,37</sup> and micro-arc oxidation treatment can reduce the degradation rate of the magnesium alloy.<sup>31</sup> Besides, polymeric-based coatings appear promising because of the diversity of chemical and physical properties. Sun et al. reported that self-assembled colloidal particles deposited onto magnesium surfaces by electrophoretic deposition method could enhance the antimicrobial properties and corrosion resistance,<sup>38</sup> and the 3DSS biomimetic peptide coating was reported to play a protective role of AZ31B in both hydrogen evolution and deposition of calcium and phosphorus.<sup>39</sup> Bazaka et al. showed that thin films of monoterpene alcohol fabricated using plasma polymerization could control Mg degradation as well as surface properties of Mg biomaterials.<sup>40</sup> In addition, laser-modified magnesium alloys have been studied in the literature, showing that the micro-nano structure on the surface of magnesium alloy prepared by lasers can effectively improve the corrosion and

bio-wettability condition.<sup>41</sup> Residual stress can also affect degradation rate. Wu et al. found that frequent closures and the angle design of staples cause surface residual stress, which affects the physiological environment of Mg corrosion behavior.<sup>22</sup>

However, knowledge of Mg alloy degradation rates is not yet complete. Most studies have focused on its use in bone tissue,<sup>35,39,42</sup> and on reducing its degradation rate. In soft tissue healing, however, we need to increase the degradation rate. Han et al. showed that the rate of Mg–Zn alloy degradation decreases in the following order:<sup>25</sup> implantation into soft tissue, trabecular bone, and cortical bone. Though it degrades faster in soft tissue,<sup>43</sup> it is still slower than what is clinically needed.

Therefore, our research group developed a novel binary Mg–2% Zn (mass fraction) (Mg–2Zn) based alloy with good tensile strength and toughness. The aims of this study were to develop a suitable sutured magnesium pin design that can not only maintain a certain mechanical strength at the initial stage, but also degrade in a short time, and to evaluate whether the Mg–2Zn alloy might be a promising candidate for use in oral wound closers in modern general surgery, thus laying a foundation for the design of oral staplers.

## Materials and methods

### Material sources

The materials, Mg–2Zn alloy with four different dimensions and designs, were acquired from Jingjun Materials Technology Co., Ltd. (Suzhou, China) and the biocompatibility and safety in vivo were verified by extensive studies.<sup>28,44,45</sup> The Mg–2Zn alloy was fabricated by smelting at 700–750°C in a high-purity graphite crucible, after stirring for 30 min, the melt was cast into a steel mold at around 700°C. A protective cover gas (a mix of carbon dioxide and sulfur hexafluoride) was employed throughout the processes. The Mg–2Zn alloys were solid-solution treated at about 350°C for 2 h. Then the heat-treated alloy sample was hot extruded at about 280°C with an extrusion ratio of 11:1, and multi-pass drawing was applied to make samples with different diameters. Finally, the samples were cut into pins with a length of 20 mm. Special molds were used to make pins with the cross-section shape of a triangle.

### Animal sources

All Sprague–Dawley (SD) male rats were from Peking University Health Science Department and had weights ranging from 180 to 220 g.

### Ethical approval

The protocols involving animals were approved by the Biomedical Ethics Committee of Peking University (pro-

ocol no. LA2017281). All animals were raised under standard conditions and were treated according to the National Institutes of Health Laboratory Animal Care and Use Guidelines.

### Magnesium pin design

The pin length was set at 20 mm for the convenience of strength measurement tests. The pins were divided into different groups based on magnesium cross-section shape, diameter, and implantation duration, as detailed in Table 1. The cross-section shapes and diameters of four different designs are shown in Figure 1. In terms of the cross-sectional area, groups 30, 31, 32, 33, and 34 and groups 40, 41, 42, 43, and 44 were designed the same. The diameter of the triangle groups was considered to be 0.3 mm. The roughness of these samples (mean value  $\pm$  SD) was  $0.172 \pm 0.0167 \mu\text{m}$  ( $n = 10$ ).

### Animal operations

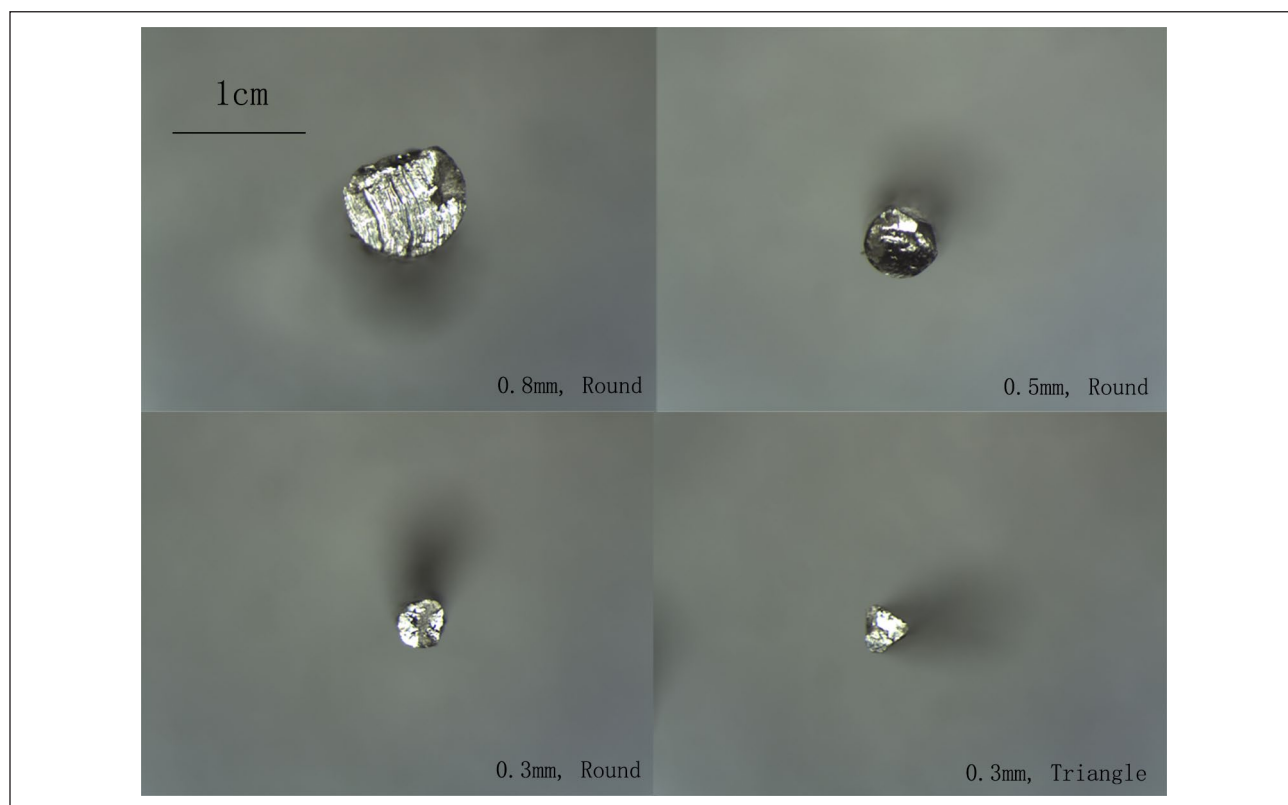
SD male rats were anesthetized using chloral hydrate through intraperitoneal injection. An iodophor was utilized to sterilize the incisions. The pins were sterilized by ultrasonic wash in acetone, ethanol, and distilled water for 15 min. Prior to animal experiments, the samples were sterilized again with surgical instruments in 0.1 MPa, 121°C for 15 min. Both right and left legs were incised respectively through two micro-incisions of 1 mm. Magnesium pins of different designs were inserted into four sites in the leg muscle and the incisions were closed with 4–0 absorbable sutures. The pins were removed after four different time periods: 1, 2, 3, and 4 weeks. Each group was repeated six times.

### Mechanical properties assessment

Mechanical properties of the pins were measured under bending test to determine flexural deformation resistance. A three-point bending test was performed in a universal testing machine (3367, Instron). The samples with different diameters (0.3, 0.5, and 0.8 mm)  $\times$  20 mm lengths were positioned on two metal supports with radii of 1 mm and a distance of 10 mm between them. When the pin was curved, the convexity was downward, and when the triangle groups were placed, the side of triangle was downward and the angle was upward. The bending punch was located in the middle between the supports. The bending punch was then moved downwards at a cross-head constant speed of 1 mm/min. The load was applied at the two contact points of each pin until plastic deformation occurred or a position 2 mm downwards from its initial position was reached. Bending stress–strain curves were obtained for each pin and compared to each other. An initial state was adjusted in which a preload of 0 N was applied to the implant. Stiffness was measured from the stress–strain

**Table I.** Groups divided by magnesium cross-section shape, diameter, and implant duration.

Group	Diameter (mm)	Cross-section shape	Implantation duration (weeks)
10	0.8	Round	0
11	0.8	Round	1
12	0.8	Round	2
13	0.8	Round	3
14	0.8	Round	4
20	0.5	Round	0
21	0.5	Round	1
22	0.5	Round	2
23	0.5	Round	3
24	0.5	Round	4
30	0.3	Round	0
31	0.3	Round	1
32	0.3	Round	2
33	0.3	Round	3
34	0.3	Round	4
40	0.3	Triangle	0
41	0.3	Triangle	1
42	0.3	Triangle	2
43	0.3	Triangle	3
44	0.3	Triangle	4

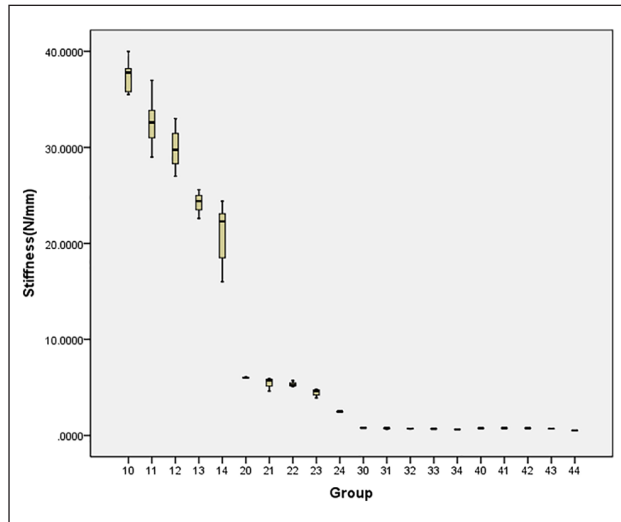
**Figure I.** The cross-section shapes and diameters of four different designs studied using a stereo microscope.

curves. Stiffness is a measure of the elasticity of a material and reflects the tendency of a material to deform

irreversibly before breakage. An average and standard deviation of six measurements were taken for each group.

**Table 2.** The mean values  $\pm$  SDs of stiffness (N/mm) in different groups.

Diameter (mm) and cross-section shape	Implant duration (weeks)				
	0	1	2	3	4
0.8, Round	37.46 $\pm$ 1.85	32.61 $\pm$ 2.65	29.88 $\pm$ 2.46	24.2 $\pm$ 1.51	20.86 $\pm$ 3.49
0.5, Round	6.03 $\pm$ 0.58	5.49 $\pm$ 0.60	5.34 $\pm$ 0.32	4.48 $\pm$ 0.40	2.47 $\pm$ 0.06
0.3, Round	0.79 $\pm$ 0.02	0.73 $\pm$ 0.08	0.71 $\pm$ 0.06	0.69 $\pm$ 0.03	0.64 $\pm$ 0.02
0.3, Triangle	0.75 $\pm$ 0.02	0.76 $\pm$ 0.03	0.76 $\pm$ 0.02	0.71 $\pm$ 0.04	0.51 $\pm$ 0.04

**Figure 2.** Box plot of stiffness in different groups.

To determine the initial stiffness for each material, six pins of each alloy were tested in their initial state.

### Surface morphology assessment

Pins were cleaned by acetone, ethanol, and distilled water ultrasonically. A 200 g/L CrO<sub>3</sub> solution was used to remove the corrosion products. Degradation surface morphologies were evaluated using a scanning electron microscope (SEM, Phenom XL, NL) before and after removal of corrosion products at the first, second, third, and fourth week after operation. Samples were also imaged and analyzed using energy-dispersive spectroscopy (EDS, Phenom XL, Netherlands) to conduct elemental analysis before removal of corrosion products.

### Statistical analysis

Statistical analysis was performed using the SPSS 19.0 software package (SPSS Inc., Chicago, IL, USA). The experimental values were expressed as mean values  $\pm$  SD. One-way analysis of variance (ANOVA) was performed to determine the differences between groups for each evaluated parameter at each time point. Non-parametrical tests ( $\kappa$

independent samples tests (Kruskal–Wallis test)) were calculated when equal variances were not assumed in one-way ANOVA. The level of significance was defined as  $p < 0.05$ .

## Results

### General condition of experimental animals

All rats grew normally and maintained regular activities and diets. There was no infection, swelling, or any other diseases that occurred throughout the experimental periods, except in two cases where the rats died three days after operation because of over-bleeding and physical weakness.

### Mechanical strength

The bending strengths (stiffness) of the pins are listed in Table 2. All four groups maintained high strengths after four weeks. The comparison of stiffness between different groups is shown in Figure 2. One-way ANOVA shows that there were significant differences between the different dimensions ( $p < 0.05$ ) and that there were significant differences between the different times in groups 10, 11, 12, 13, and 14 and groups 20, 21, 22, 23, and 24 ( $p < 0.05$ ). However, there was no significant difference between the different times in groups 30, 31, 32, 33, and 34 and groups 40, 41, 42, 43, and 44. There was also no significant difference between the groups with different shape but the same dimensions in groups 30 and 40, 31 and 41, 32 and 42, 33 and 43, and 34 and 44.

### Scanning electron microscope evaluation

The samples extracted after different implantation times were dried and imaged using backscatter electron detection (BSD) to assess the corrosion products formed. The surface morphologies showed that there were many precipitates and cracks on the surfaces. It was observed that the degree of Mg–2Zn pin substrates corrosion was proportional to the implantation time (Figure 3).

The elemental energy spectrum analyses of the components of corrosion products (Table 3) were conducted. There were no significant differences in the elemental compositions of different groups. However, composition ratios

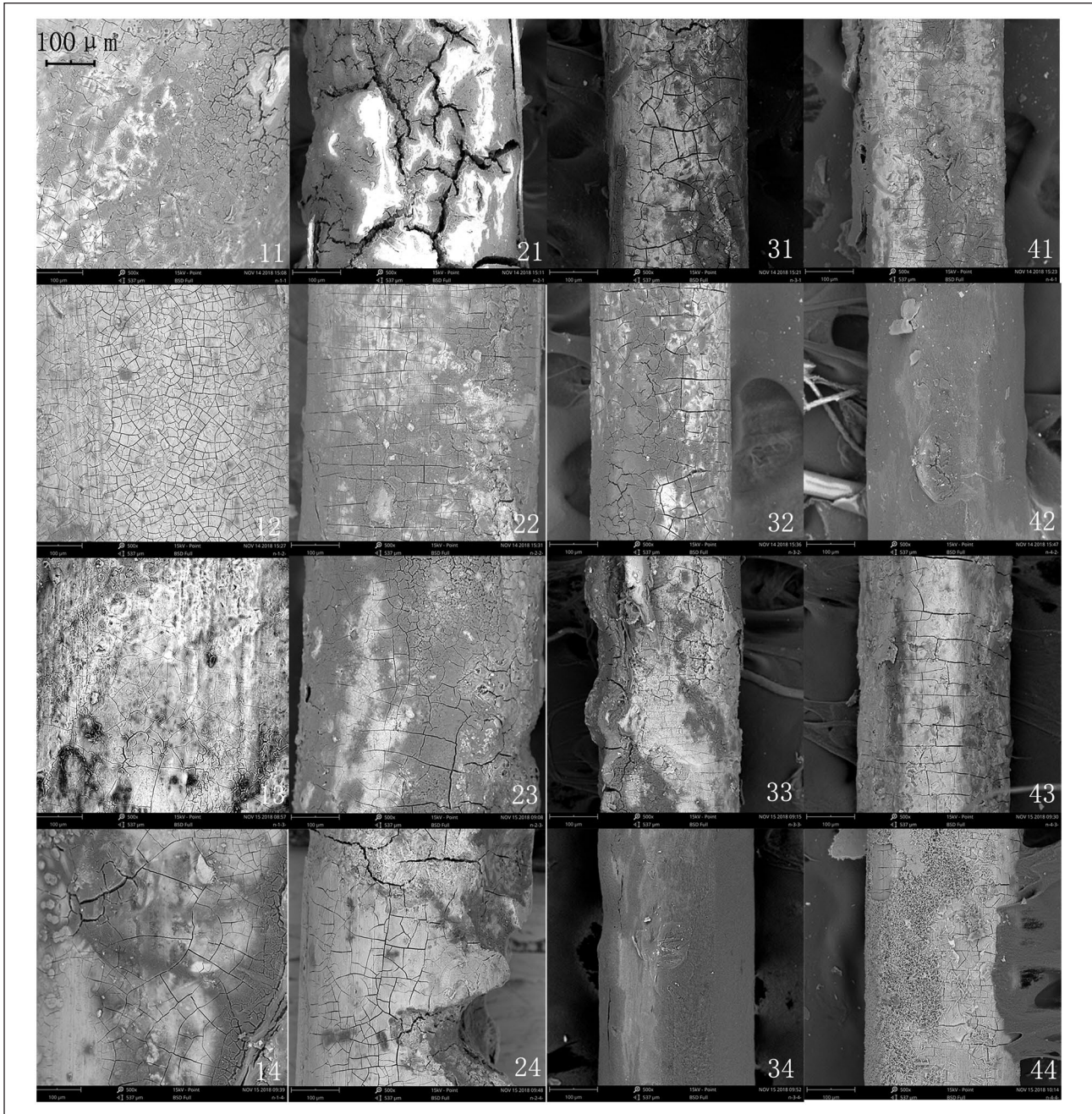


**Figure 3.** The corrosion surfaces of Mg–2Zn pins in different groups using BSD.

varied in different areas of the pins. After *in vivo* corrosion, corrosion products and layers rich in Mg, P, and Ca were observed to have formed on the alloy surface. The agglomerates of corrosion deposits contained high Ca and P content. Some areas showed large amounts of elements such as C, N, Na, and K. There were small areas rich in Zn, which may prove the existence of MgZn phases that are more resistant to corrosion. In group 44, we saw a large amount of rod-like crystals on the surface that contained mostly P, which may prove the formation of phosphate.

After the removal of corrosion products, we used the secondary electron detector (SED) to observe the surface

topography. This revealed widespread corrosion that resulted in irregular and porous surface topographies in all groups (Figure 4). The number, dimension, and range of holes and defect volumes showed the degrees of corrosion. In the groups 14, 24, 34, and 44, there was significantly greater corrosion in that some parts of the pins became very thin and almost broke.

## Discussion

The development of a biodegradable magnesium pin stapler has several advantages. The biodegradable magnesium matrix material avoids the need to remove the pin and

**Table 3.** Elemental energy spectrum analysis of the components of corrosion products (wt %).

Group	Mg	Ca	P	Na
11	14.76	44.95	40.29	
21	23.83	31.15	35.47	9.55
31	29.79	29.9	40.3	
41	53.55	21.61	19.69	5.15
12	39.2	23.34	37.46	
22	55.24	16.21	28.55	
32	17.67	42.46	39.87	
42	14.5	51.22	34.28	
13	24.65	44.47	30.88	
23	11.43	52.87	35.7	
33	18.39	48.23	33.39	
43	90.37	6.41	3.22	
14	25.63	36.34	38.03	
24	27.77	40.89	31.34	
34	22.41	37.55	40.04	
44	49.4	1.98	48.62	

reduces the secondary pain of the patient. The pin has a good initial mechanical strength, Cho et al. reported that the initial strength of Mg–Ca–Zn alloy was higher than those of biostable and biodegradable polymers,<sup>46</sup> which shows it might be suitable for gastrointestinal mucosa,<sup>22</sup> vocal cord, muscle, scalp, and other parts of high-tension tissue. A stapling device can be used to sew conveniently, and the pin can be combined with femtosecond laser automatic cutting and applied to automatic surgical robots for automatic stitching. This reduces the burden and error of manual operation and addresses the difficult problem of deep maneuvering in a small space. Thus, it will greatly improve the efficiency of deep and narrow space suture.

We tried to implant the pins into the rats' tongues, but because of the mechanical test length requirement (a length of over 15 mm must be used), all of the rats spat out the pins from the crevice in the suture a day after insertion. This may be because the pin size was too big for the rats' tongues, the wound site was hard to close tightly, and tongue movement is flexible in rats. However, in our previous experience, we inserted shorter pins with length of 5 mm in the tongue and checked the tissue reaction, there were no obvious inflammation and the degradation rates did not vary in comparison to the leg muscle.

There were small lumps of gas bubbles surrounding the pins in some muscle tissue due to products from magnesium degradation. Recent basic and clinical studies have found that an appropriate amount of hydrogen plays an active role in maintaining the normal functions of the central nervous system, respiratory system, and digestive system.<sup>11</sup> The alkalinity induced by abundant hydroxides and hydrogen might also damage the surrounding tissue.<sup>20</sup> However, no obvious inflammation or systemic adverse reaction was observed in this study.

Adequate mechanical properties are important to ensure that the wound does not open. We used stiffness to measure

the bending strengths because the samples were not of standard dimensions, which are required for modulus of elasticity measurements. The stiffness shows the bending strength per strain unit, which reveals the resistance to deformation and wound closure stability with tension in the wound. In our results, the stiffness varied significantly between pins with different dimensions. The 0.8 mm pin showed a very high strength, but in practice, the 0.8 mm pin is too big for sutures, has a very slow degradation rate, and causes obvious discomfort. The 0.3 mm pin is very fragile and easily transformed, while the 0.5 mm pin guarantee sufficient strength. Thus, a dimension between 0.3 mm to 0.5 mm is more likely to be a suitable size. The stiffness also varied significantly between the different times in groups 10, 11, 12, 13, and 14 and groups 20, 21, 22, 23, and 24 but no significant difference between the different times in groups 30, 31, 32, 33, and 34 and groups 40, 41, 42, 43, and 44, these probably due to the drop of stiffness was more obvious when the stiffness was high. But at least it showed the stiffness was relatively stable within the first week which is critical for wound healing.

There were no significant differences of stiffness between the two shapes with the same dimensions, but there might be some advantages to the triangle shape over the round shape. In clinical use, a triangular-headed suture needle is more penetrating than a round-headed suture needle. Thus, in future use, a triangle shape might be easier for penetrating tissues.

There were large topography differences before and after removing corrosion products. Before removing the corrosion, the surfaces were relatively complete and covered by corrosion products, and there were many evenly distributed cracks. After removing the corrosion, porous pits of different sizes were revealed. Small pits were due to the crystal corrosion started from the Mg matrix. Large pits were probably due to small amounts of corrosion

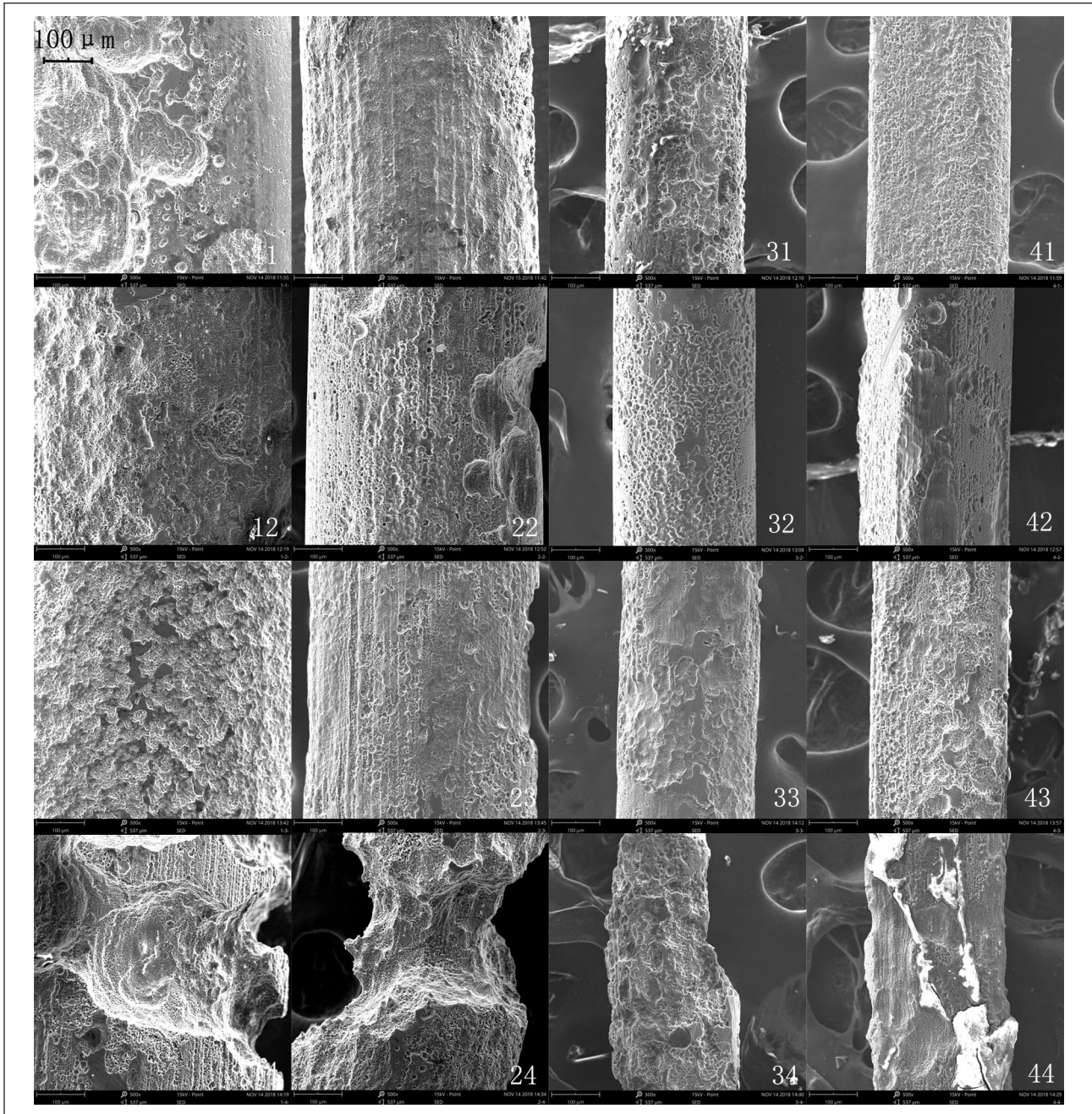


**Figure 4.** Surface characteristics after removing the corrosion product analyzed with the SED. Removal of corrosion products revealed widespread corrosion resulting in irregular surface topographies on all groups.

around the margin of some dots, such as MgZn phases, or small pit corrosion spreading to deeper or surrounding areas and leading to a large chunk dropping out from the material. The corrosion forms were the same between different groups, since all four different designs came from same composition, but the corrosion pits were smaller and denser with increased degradation times. We observed some largely corroded areas in the pins, like a ring which led to locally extremely narrow and easily fractured area. The probable reasons for this were inner strength when

processed; the micro environmental factors in vivo like temperature and fluid exchange; rat muscle movement; the uneven composition of different phases; or the formation of cracks, which caused a stress concentration.

Elemental compositions varied in different areas of the pins. The agglomerates of corrosion deposits contained rich Ca and P content. Marques et al. showed that higher Ca/P on a Ti surface can improve surface features and biofunctions.<sup>47</sup> Thus, this may indirectly prove the biocompatibility of this composition. Some areas that showed rich amounts of

elements such as C, N, Fe, Na, and K were considered to be covered with blood, muscle tissue, or organic remnants. There were dots rich in Zn, which may prove the existence of MgZn phases that seemed to be more resistant to corrosion. This might be the reason why dots stay complete while the surrounding Mg matrix was largely corroded. In group 44, we saw a large amount of rod-like crystals on the surface, which contained mostly P, possibly proving the formation of phosphate. It is critical to clean off the blood, body fluid, and muscle tissue before saving the samples due to the probable interference of protein in blood or some muscle tissue that may lead to elemental composition error.

The degradation rate is a critical factor. Too quick of a degradation rate will lead to increasing alkalinity of the local environment,<sup>48</sup> local inflammation, and will make it difficult to meet the strength requirement. Too slow of a degradation rate will cause the pin to become a foreign body. In our study, the degradation of Mg–2Zn was slow, and there were still large parts of the pins that were not degraded after 4 weeks post-implantation. The wound would have been healed at this rate, and the foreign body is still inside, thus inducing uncomfortable symptoms and influencing regular movement. The degradation rate is influenced by many factors, including the alloying elements and microstructure, the rats' movement, the body fluid environment such as serum protein,<sup>49</sup> the presence or absence of a surface oxide layer, processing error, and so on. It is critical to accelerate the degradation rate in our future studies.

## Conclusion

In conclusion, the bending strengths and degradation rates over different time periods of Mg–2Zn pins in rats' leg muscle were investigated and compared. A dimension around 0.5 mm is a suitable size for their application and mechanical requirements, but the degradation rate needs to be improved. We proved that a magnesium alloy pin is likely to be a promising candidate for stapler pins for oral mucosa, tongue, and larynx wound closers. We will further improve the properties and compositions of the magnesium alloy to accelerate the degradation rate and cooperate with an independently developed robot for oral and larynx surgery to realize automatic magnesium stapler sutures.

## Declaration of Conflicting Interests

The author(s) declared no potential conflicts of interest with respect to the research, authorship, and/or publication of this article.

## Funding

The author(s) disclosed receipt of the following financial support for the research, authorship, and/or publication of this article: This work was supported by the National Natural Science Foundation of China (Grant Number 81571023), State Key Lab of Advanced Metals and Materials (Grant Number 2018-Z04), and Clinical Medicine Plus X – Young Scholars Project of Peking University (Grant Number PKU2019LCXQ024).

## ORCID iD

Wenjun Li  <https://orcid.org/0000-0002-7594-5442>

## References

1. Madani M, Berardi T and Stoopler ET. Anatomic and examination considerations of the oral cavity. *Med Clin North Am* 2014; 98: 1225-1238.
2. Chen D, Song J, Zhao Y, et al. Systematic review and meta-analysis of surgical zipper technique versus intracutaneous sutures for the closing of surgical incision. *PLoS One* 2016; 11: e0162471.
3. Bahouth Z, Halachmi S, Shprits S, et al. The use of bovine serum albumin–glutaraldehyde tissue adhesive (BioGlue(R)) for tumor bed closure following open partial nephrectomy. *Actas Urol Esp* 2017; 41: 511-515.
4. Reilly WT, Pemberton JH, Wolff BG, et al. Randomized prospective trial comparing ileal pouch-anal anastomosis performed by excising the anal mucosa to ileal pouch-anal anastomosis performed by preserving the anal mucosa. *Ann Surg* 1997; 225: 666-677.
5. Feese CA, Johnson S, Jones E, et al. A randomized trial comparing metallic and absorbable staples for closure of a Pfannenstiel incision for cesarean delivery. *Am J Obstet Gynecol* 2013; 209: 556-e1.
6. Nitsche J, Howell C and Howell T. Skin closure with subcuticular absorbable staples after cesarean section is associated with decreased analgesic use. *Arch Gynecol Obstet* 2012; 285: 979-983.
7. Seitz JM, Durisin M, Goldman J, et al. Recent advances in biodegradable metals for medical sutures: a critical review. *Adv Healthcare Mater* 2015; 4: 1915-1936.
8. Asgari M, Hang R, Wang C, et al. Biodegradable metallic wires in dental and orthopedic applications: a review. *Metals* 2018; 8: 212.
9. Wang J, Xu J, Liu W, et al. Biodegradable magnesium (Mg) implantation does not impose related metabolic disorders in rats with chronic renal failure. *Sci Rep* 2016; 6: 26341.
10. Lin DJ, Hung FY, Yeh ML, et al. Microstructure-modified biodegradable magnesium alloy for promoting cytocompatibility and wound healing in vitro. *J Mater Sci Mater Med* 2015; 26: 248.
11. Zhao D, Wang T, Nahan K, et al. In vivo characterization of magnesium alloy biodegradation using electrochemical H2 monitoring, ICP-MS, and XPS. *Acta Biomater* 2017; 50: 556-565.
12. Chou D-T, Hong D, Saha P, et al. In vitro and in vivo corrosion, cytocompatibility and mechanical properties of biodegradable Mg–Y–Ca–Zr alloys as implant materials. *Acta Biomater* 2013; 9: 8518-8533.
13. Zberg B, Uggowitzer PJ and Löffler JF. MgZnCa glasses without clinically observable hydrogen evolution for biodegradable implants. *Nat Mater* 2009; 8: 887-891.
14. Okawachi H, Ayukawa Y, Atsuta I, et al. Effect of titanium surface calcium and magnesium on adhesive activity of epithelial-like cells and fibroblasts. *Biointerphases* 2012; 7: 27.
15. Persaud-Sharma D and McGoron A. Biodegradable magnesium alloys: a review of material development and applications. *J Biomim Biomater Tissue Eng* 2012; 12: 25-39.

16. Yoshida T, Fukumoto T, Urade T, et al. Development of a new biodegradable operative clip made of a magnesium alloy: evaluation of its safety and tolerability for canine cholecystectomy. *Surgery* 2017; 161: 1553-1560.
17. Moravej M and Mantovani D. Biodegradable metals for cardiovascular stent application: interests and new opportunities. *Int J Mol Sci* 2011; 12: 4250-4270.
18. Ikeo N, Nakamura R, Naka K, et al. Fabrication of a magnesium alloy with excellent ductility for biodegradable clips. *Acta Biomater* 2016; 29: 468-476.
19. Chaya A, Yoshizawa S, Verdalis K, et al. Fracture healing using degradable magnesium fixation plates and screws. *J Oral Maxillofac Surg* 2015; 73: 295-305.
20. Yu K, Dai Y, Luo Z, et al. In vitro and in vivo evaluation of novel biodegradable Mg–Ag–Y alloys for use as resorbable bone fixation implant. *J Biomed Mater Res Part A* 2018; 106: 2059-2069.
21. Wang J, Xu J, Fu W, et al. Biodegradable magnesium screws accelerate fibrous tissue mineralization at the tendon-bone insertion in anterior cruciate ligament reconstruction model of rabbit. *Sci Rep* 2017; 7: 40369.
22. Wu H, Zhao C, Ni J, et al. Research of a novel biodegradable surgical staple made of high purity magnesium. *Bioact Mater* 2016; 1: 122-126.
23. Chng CB, Lau DP, Choo JQ, et al. A bioabsorbable micro-clip for laryngeal microsurgery: design and evaluation. *Acta Biomater* 2012; 8: 2835-2844.
24. Li B, Yang K and Wang X. Biodegradable magnesium wire promotes regeneration of compressed sciatic nerves. *Neural Regen Res* 2016; 11: 2012-2017.
25. Han P, Cheng P, Zhang S, et al. In vitro and in vivo studies on the degradation of high-purity Mg (99.99wt.%) screw with femoral intracondylar fractured rabbit model. *Biomaterials* 2015; 64: 57-69.
26. Lau DP, Chng CB, Choo JQ, et al. Development of a micro-clip for laryngeal microsurgery: initial animal studies. *Laryngoscope* 2012; 122: 1809-1814.
27. Wang B, Yan L, Huo W, et al. Rare earth elements and hypertension risk among housewives: a pilot study in Shanxi Province, China. *Environ Pollut* 2017; 220: 837-842.
28. Fazel Anvari-Yazdi A, Tahermanesh K, Hadavi SM, et al. Cytotoxicity assessment of adipose-derived mesenchymal stem cells on synthesized biodegradable Mg–Zn–Ca alloys. *Mater Sci Eng C* 2016; 69: 584-597.
29. Lai H, Li J, Li J, et al. Effects of Sr on the microstructure, mechanical properties and corrosion behavior of Mg–2Zn–xSr alloys. *J Mater Sci Mater Med* 2018; 29: 87.
30. Zhou YL, Li Y, Luo DM, et al. Microstructures, mechanical and corrosion properties and biocompatibility of as extruded Mg–Mn–Zn–Nd alloys for biomedical applications. *Mater Sci Eng C* 2015; 49: 93-100.
31. Lin X, Tan L, Wang Q, et al. In vivo degradation and tissue compatibility of ZK60 magnesium alloy with micro-arc oxidation coating in a transcortical model. *Mater Sci Eng C* 2013; 33: 3881-3888.
32. Yan J, Chen Y, Yuan Q, et al. Comparison of the effects of Mg–6Zn and Ti–3Al–2.5V alloys on TGF-beta/TNF-alpha/VEGF/b-FGF in the healing of the intestinal tract in vivo. *Biomed Mater* 2014; 9: 025011.
33. Wang X, Ni J, Cao N, et al. In vivo evaluation of Mg–6Zn and titanium alloys on collagen metabolism in the healing of intestinal anastomosis. *Sci Rep* 2017; 7: 44919.
34. Uddin MS, Hall C and Murphy P. Surface treatments for controlling corrosion rate of biodegradable Mg and Mg-based alloy implants. *Sci Technol Adv Mater*. 2015; 16: 053501.
35. Tan L, Wang Q, Lin X, et al. Loss of mechanical properties in vivo and bone-implant interface strength of AZ31B magnesium alloy screws with Si-containing coating. *Acta Biomater* 2014; 10: 2333-2340.
36. Hornberger H, Virtanen S and Boccaccini AR. Biomedical coatings on magnesium alloys: a review. *Acta Biomater* 2012; 8: 2442-2455.
37. Bakhsheshi-Rad HR, Hamzah E, Kasiri-Asgarani M, et al. Deposition of nanostructured fluorine-doped hydroxyapatite-polycaprolactone duplex coating to enhance the mechanical properties and corrosion resistance of Mg alloy for biomedical applications. *Mater Sci Eng C* 2016; 60: 526-537.
38. Sun J, Zhu Y, Meng L, et al. Electrophoretic deposition of colloidal particles on Mg with cytocompatibility, antibacterial performance, and corrosion resistance. *Acta Biomater* 2016; 45: 387-398.
39. Cui W, Beniash E, Gawalt E, et al. Biomimetic coating of magnesium alloy for enhanced corrosion resistance and calcium phosphate deposition. *Acta Biomater* 2013; 9: 8650-8659.
40. Bazaka K, Ketheesan N and Jacob MV. Polymer encapsulation of magnesium to control biodegradability and biocompatibility. *J Nanosci Nanotechnol* 2014; 14: 8087-8093.
41. Ho YH, Vora HD and Dahotre NB. Laser surface modification of AZ31B Mg alloy for bio-wettability. *J Biomater Appl*. 2015; 29: 915-928.
42. Sun W, Zhang G, Tan L, et al. The fluoride coated AZ31B magnesium alloy improves corrosion resistance and stimulates bone formation in rabbit model. *Mater Sci Eng C* 2016; 63: 506-511.
43. Henderson SE, Verdalis K, Maiti S, et al. Magnesium alloys as a biomaterial for degradable craniofacial screws. *Acta Biomater* 2014; 10: 2323-2332.
44. Gong H, Wang K, Strich R, et al. In vitro biodegradation behavior, mechanical properties, and cytotoxicity of biodegradable Zn–Mg alloy. *J Biomed Mater Res Part B* 2015; 103: 1632-1640.
45. Gu X, Zheng Y, Cheng Y, et al. In vitro corrosion and biocompatibility of binary magnesium alloys. *Biomaterials* 2009; 30: 484-498.
46. Cho SY, Chae SW, Choi KW, et al. Biocompatibility and strength retention of biodegradable Mg–Ca–Zn alloy bone implants. *J Biomed Mater Res Part B* 2013; 101: 201-212.
47. Marques Ida S, da Cruz NC, Landers R, et al. Incorporation of Ca, P, and Si on bioactive coatings produced by plasma electrolytic oxidation: the role of electrolyte concentration and treatment duration. *Biointerphases* 2015; 10: 041002.
48. Johnson I and Liu H. A study on factors affecting the degradation of magnesium and a magnesium-yttrium alloy for biomedical applications. *PLoS One* 2013; 8: e65603.
49. Johnson I, Jiang W and Liu H. The effects of serum proteins on magnesium alloy degradation in vitro. *Sci Rep* 2017; 7: 14335.